Spectral and temporal properties of X-ray emission from the ultra-luminous source X-9 in M81

V. La Parola, Universitá di Palermo; **G. Fabbiano**, Smithsonian CfA, Cambridge (MA); **D.W. Kim**, Smithsonian CfA, Cambridge (MA); **G. Peres**, Universitá di Palermo.

Abstract

We have analysed the spectra and the variability of individual X-ray sources in the M-81 field using data from the available ROSAT-PSPC and ROSAT-HRI observations of this nearby spiral galaxy.

Here we present the results on the second brightest source in the field (X-9 - Fabbiano, 1988 ApJ 325 544), whose identification and interpretation is still unclear. Our work includes the study of the shape of X-9 from HRI data, the light curve and hardness ratio evolution, and the spectral analysis.

1 Fundamental characteristics

X9-M81, a very bright X-ray source, is located 12.5' far from M81 nucleus, at coordinates 09h 57m 54s +69 03' 48" (J2000). It was first detected with Einstein and, since then many hypotheses have been made on its nature, also on the basis of the very high X-ray luminosity (more than 10^{39} if at the distance of M 81). The most important ones are:

- an extended structure (a super-shell) heated by the detonation of many (> 50) supernovae (Miller 1995)
- a compact object (WD, NS or BH) accreting material from a dense cloud of interstellar gas (Miller 1995)
- a background quasar (Ishisaki et al. 1996)

Some important issues, that make understanding this object even more difficult concern its optical appearance and its position. X-9 optical counterpart is not well identified: the only candidate so far is a weak (probably extended) object of $m_B \sim 19$. Moreover, the source appears to be isolated, well outside the M81 optical image and there is no evident association with other galaxies in the group, albeit it may belong to the outskirts regions of the HoIX dwarf galaxy.

2 The data

We analysed the available archival data from ROSAT PSPC (12 observation, with 8 pointed on M 81 nucleus for a total exposure time of 146 ksec) and HRI (7 observations pointed on M 81 nucleus for a total exposure time of 135 ksec). We also used a SAX observation pointed on M 81 and one ASCA observation pointed on X-9.

instr.	ref	sequence nr	live time	start date	off axis
ROSAT PSPC	1P	rp600101a00	9296	25/03/91	12.5'
	2P	rp600110a00	12717	27/03/91	38.0'
	3P	rp600052n00	6588	18/04/91	31.2'
	4P	rp600110a01	12238	15/10/91	38.0'
	5P	rp600101a01	11085	16/10/91	12.5'
	6P	rp600382n00	27120	29/09/92	12.5'
	7P	rp180015n00	17938	03/04/93	12.5'
	8P	rp180015a01	8731	04/05/93	12.5'
	9P	wp600576n00	16412	29/09/93	32.0'
	10P	rp180035n00	17800	01/11/93	12.5'
	11P	rp180035a01	4234	07/11/93	12.5'
	12P	rp180050n00	1849	31/03/94	12.5'
ROSAT HRI	1H	rh600247n00	26320	23/10/92	12.5'
	2H	rh180015n00	1688	16/04/93	12.5'
	3H	rh600247a01	21071	17/04/93	12.5'
	4H	rh600739n00	19902	19/10/94	12.5'
	5H	rh600740n00	18984	13/04/95	12.5'
	6H	rh600881n00	14826	12/10/95	12.5'
	7H	rh601002n00	19776	30/09/97	12.5'
	8H	rh601095n00	12590	25/03/98	12.5'
BeppoSAX	MECS	40732001	100287	04/06/98	13'
	LECS		43931		
ASCA	SIS	57048000	33000	06/04/99	-

Table 1: Log of ROSAT, SAX, ASCA observation of X-9. Sequence 2H has not used for this work.

Figure 1: **fig1-left.jpg** : contour plots of X-ray count rates, superimposed to the optical image of M81 field. X-9 is marked by an arrow. **fig1-right.jpg**: Enlargement of the region within the box in the upper panel shows both the position of X-9 with respect to Holmberg IX and the faint optical source coincident with the X-ray emission centroid

3 Spatial structure of the X-ray emission

The X-9 radial profile derived from HRI observations has been compared with that of an HRI calibration source (HZ43) observed at the same off axis angle. As the calibration profile is visibly asymmetric, we divided the source image into two pie slices (external/internal, see Figure 2) with respect to the direction of the detector center. In the figure, X-9 has been rotated to have the same orientation has the calibration source. We derived the radial profile for each slice both for the calibration source and for X-9. Figure 3 shows the radial profile along the two directions. The right panel shows that X-9 (diamonds) has a significant emission excess between 10 and 25 arcsec away from the center with respect to the calibration source (stars).
HRI data then suggest a very bright point-like source but also the presence of an extended component.

Figure 2: **fig2-up.jpg. Left**: contour plot of HZ43 counts in a ROSAT HRI image at 12 arcmin off axis. Note the asymmetric structure of the PSF. **Right**: contour plot of X-9 counts, rotated to have the same position as HZ43 with respect to the detector center. Sectors used for the radial profile extraction are also shown.

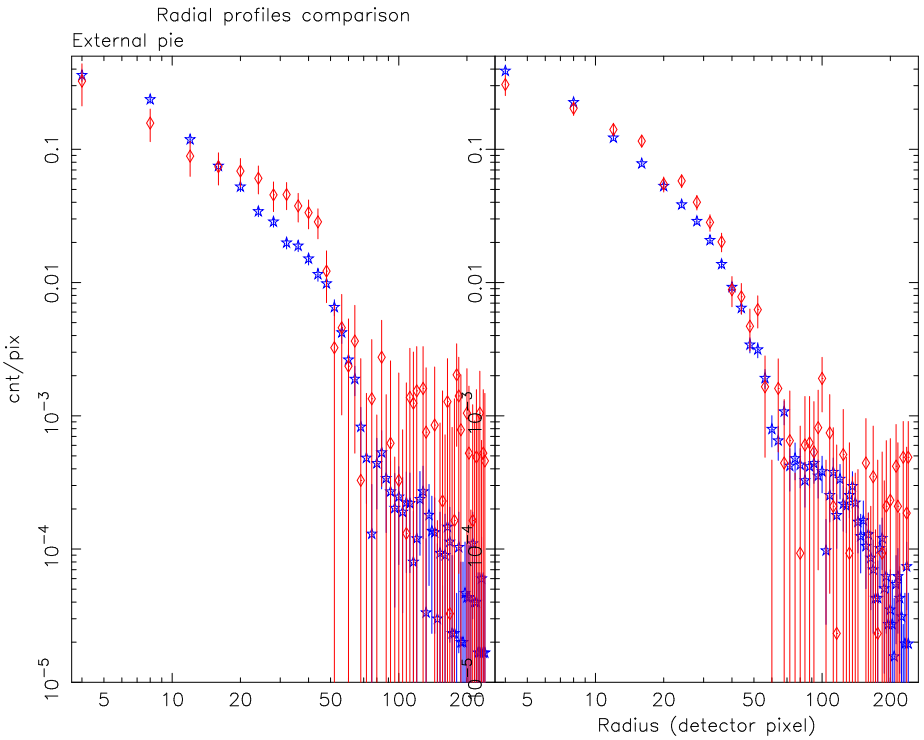

Figure 3: Radial profiles of the calibration source HZ43 (stars), compared to X-9 profile (diamonds). Left panel: external sector. Right panel: internal sector. Data points are normalized to the total number of counts within 2 arcmin. Extraction annuli are 2 arcsec wide (1 detector pixel = 0.5 arcsec)

4 Source variability

For each observation we calculated the source flux in the [0.5-2.4] keV energy band using the parameters that best fit the PSPC spectra (see next Section) Results are reported in Figure 4, where each data point corresponds to one individual observation. Here we note that, in spite of the fact that they are taken with different instruments, HRI and PSPC data are in good agreement, and this is particularly evident in the period that covers April 1992. Moreover SAX data are consistent with the trend shown by the last HRI observations, while the ASCA point shows a much higher emission. The source flux is clearly variable: variability on time scales of months as well as a descending trend on longer time scale are evident in Figure 4. The data do not show any hint of periodical variability. A flare or a change in the physical status of the source could be responsible for the flux increase shown by the ASCA observation.
We also looked for spectral variability in PSPC data, by evaluating two different hardness ratios, both defined as

$$\mathrm{HR} = \frac{hard-soft}{hard+soft}$$

using the energy bands showed in Table 4. We decided to use two different definitions of hardness ratio because the second (HR2) allows us a coarse spectral analysis of the high energy part of the ROSAT/PSPC band, appropriate for harder sources. We plotted both hardness ratios in Figure 5, along with PSPC counts rate. We found very little evidence of variability, with only one point showing a softer spectrum (observation 4P).
These results seem to exclude the hypothesis of a Supernovae shell: this scenario could not explain the variability we observe unless we suppose a large number of Supernovae explosions during the seven years covered by the observing period, but no event of this kind has been observed in other wavelenght bands. Instead, the light curve points to a compact source or an AGN.

		Soft	Hard
Whole band	HR1	0.11-0.42 KeV	0.52-2.02 KeV
Hard band	HR2	0.52-0.91 KeV	0.91-2.02 KeV

Table 2: Definitions of bands used in the calculation of the two hardness ratios

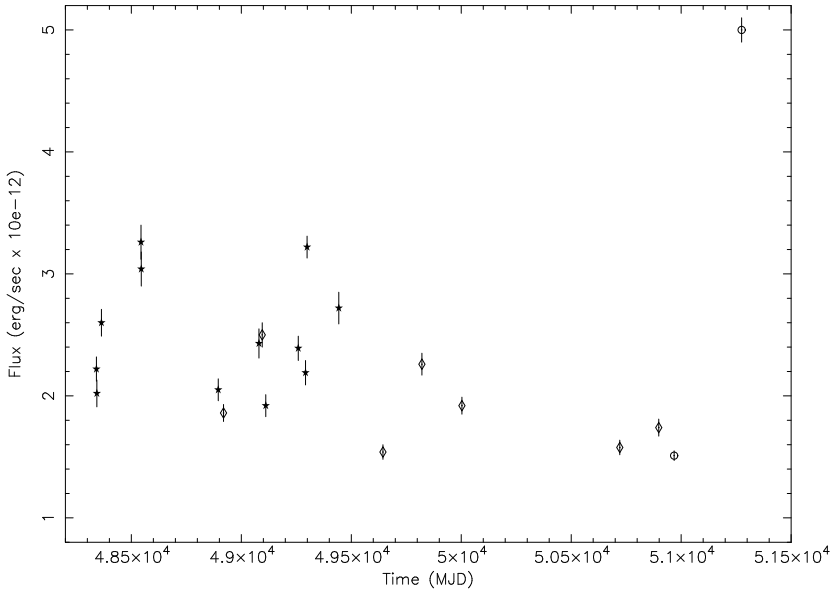

Figure 4: X-9 flux between 0.5 and 2.4 keV as a function of time. Stars are PSPC data points, diamonds are HRI data points, the two circles represent the SAX (first in time) and the ASCA data points.

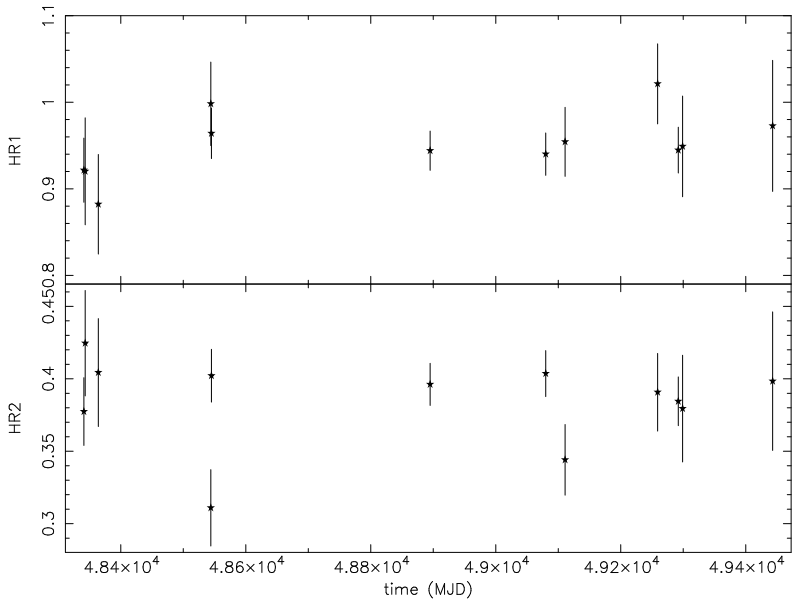

Figure 5: Hardness ratios HR1 and HR2 for X-9 in M81 from ROSAT-PSPC data. Ratios HR1 and HR2 are both defined as $\frac{hard-soft}{hard+soft}$ for different definitions of the bands, see Table 2

5 Spectral analysis

We analysed spectral data derived from ROSAT/PSPC, SAX/LECS, SAX/MECS and ASCA/SIS (GIS data were not used because of the contamination from M 81 nucleus) In order to test the different hypotheses on the nature of X-9 we used the following models:

- an absorbed power-law (implying the hypothesis of a quasar or of a compact object);
- a Raymond spectrum with one or two temperatures (related to the super-shell hypothesis);
- a multi-color black body disk (MCBB - adequate to a black hole hypothesis - Makishima et al., 2000).

The Raymond model fails to fit the observed spectra. The best fit results are shown in Table 3. Here we note that while SAX/LECS and ROSAT spectra appear very similar (in both cases the MCBB best fit has been obtained using SAX/MECS to fix the hard power-law component), ASCA data show a considerably different behaviour, with a higher temperature disk and no evidence for the presence of a power-law or of a line.

	Instruments	nH($\times 10^{22}$)	Γ	T (keV)	$E_{line}(\Delta E)$	χ^2_ν (Prob)
1	MECS	$0.04^{+0.5}$	0.85 ± 0.2	-	-	1.11 (0.27)
2	MECS	$0.04^{+0.6}$	0.92 ± 0.16	-	$6.4^{+0.5}_{-0.17}(0.43)$	1.03 (0.42)
2	MECS+LECS	$0.04^{+0.07}$	$1.12^{+0.26}_{-0.14}$	-	$6.6^{+0.3}_{-0.8}(0.99)$	1.04 (0.38)
3	MECS+LECS	$0.34^{+0.56}_{-0.26}$	$0.80^{+0.25}_{-0.40}$	$0.30^{+0.15}_{-0.12}$	$6.4^{+0.2}_{-0.6}(0.37)$	0.91 (0.66)
3	MECS+PSPC	$0.16^{+0.13}_{-0.04}$	$0.82^{+0.27}_{-0.20}$	$0.32^{+0.07}_{-0.10}$	$6.4^{+0.25}_{-1.5}(0.39)$	0.84 (0.83)
4	ASCA SIS	0.177 ± 0.015	-	1.24 ± 0.03	-	1.13(0.05)

Table 3: Spectral analysis: fit results. The first column contains the model description according to the following code: 1) Power-law; 2) Power-law + Gaussian line; 3) Power-law + MCBB + Gaussian line; 4) MCBB. The lower limit for the column density is 4.1×10^{-2}, i.e. the galactic line of sight value. Γ is the power-law index. T is the temperature of the MCBB, wherever this model has been used. The energy of the line is expressed in keV; we put within parenthesis the line equivalent width in the same units.

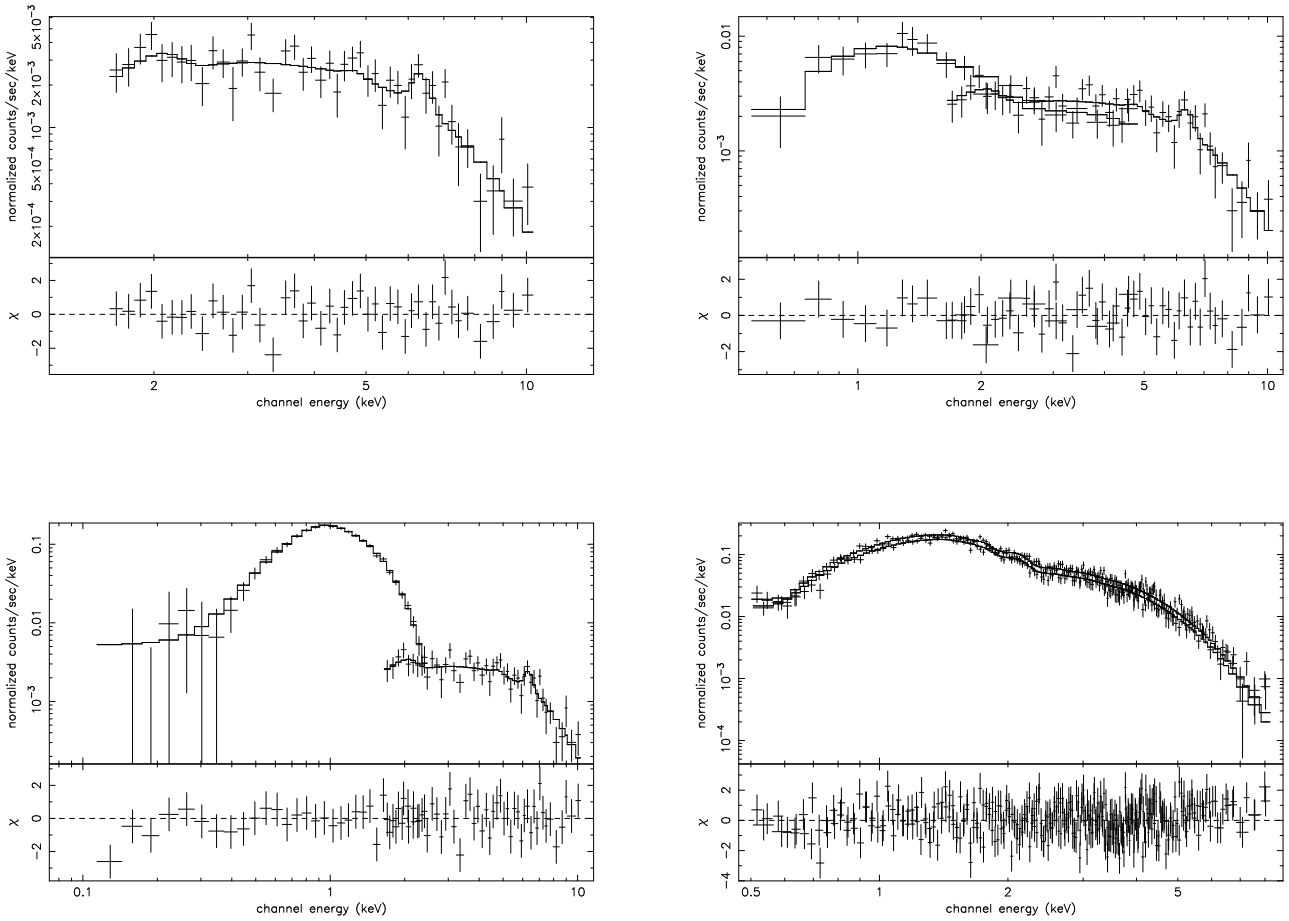

Figure 6: X-9 spectra, best fit models and residuals in χ units. Upper left: MECS (power-law + line). Upper right: MECS + LECS (power-law + MCBB + line). Lower Left: PSPC + MECS (power-law + MCBB + line). Lower right: ASCA (MCBB). The relevant parameters are in Table 3. ASCA data are from the two SIS detectors.

6 Final considerations

- HRI emission centroid is well coincident with a faint object in the POSS II image
- The source flux is strongly variable on relatively short time scales: this fact is at odds with the hypothesis of a Supernovae super shell and suggests that X-9 is a compact accreting source
- An extended component can however exist (as suggested by HRI data).
- If at M81 distance, the average X-ray luminosity of the source is $\sim 4 \times 10^{39}$ erg/sec, well above the Eddington limit for a $1M\odot$ accreting object
- The results of the spectral fitting, supporting the MCBB model, seem to confirm the Super-Eddington nature of X-9: MCBB is the model used to fit the X-ray spectrum of Super-Eddington sources, and the temperature values we find are compatible with those of Galactic Black Hole candidates (Makishima et al. 1999)
- A definite spectral variation is evident between SAX/PSPC and ASCA observations.

A more detailed description of the analysis, as well as the interpretation of the results will appear in La Parola et al. (2000), in preparation.

This work was supported in part by NASA grant NAG5-2946 and NASA contract NAS8-39073(CXC) and in part by MURST. This research has made use of the HEASARC online database and of the ESO online DSS.

7 Reference

Fabbiano G., 1988, ApJ, **325**, 544
Ishisaki Y. et al. 1996, PASJ, **48**, 237
La Parola V., Fabbiano G., Kim D.W., Peres G., Bocchino F., 2001, in preparation
Makishima K. et al. 2000, ApJ, **535**, 632
Miller B. W., 1995, ApJ, **446**, L75